

Neutron powder diffraction and magnetic study of perovskites $\text{Pb}(\text{Mn}_{1/2}\text{Nb}_{1/2})\text{O}_3$ and $\text{Pb}(\text{Mn}_{1/4}\text{Fe}_{1/4}\text{Nb}_{1/2})\text{O}_3$

S.A. Ivanov^{a,c}, P. Nordblad^b, R. Tellgren^{c,*}, H. Rundlof^c,
G. André^d, F. Bourée^d

^a Department of Inorganic Materials, Karpov' Institute of Physical Chemistry, Vorontsovo pole 10 105064, Moscow K-64, Russia

^b Department of Engineering Sciences, The Ångström Laboratory, Box 534, University of Uppsala, SE-751 21 Uppsala, Sweden

^c Department of Materials Chemistry, The Ångström Laboratory, University of Uppsala, SE-751 21 Uppsala, Sweden

^d Laboratoire Leon Brillouin, Saclay, France

Received 9 November 2007; accepted 16 November 2007

Available online 15 January 2008

Abstract

The structural and magnetic properties of the complex metal oxides $\text{Pb}(\text{Mn}_{1/2}\text{Nb}_{1/2})\text{O}_3$ (PMNO) and $\text{Pb}(\text{Mn}_{1/4}\text{Fe}_{1/4}\text{Nb}_{1/2})\text{O}_3$ (PMFNO), which belong to a class of disordered perovskites have been studied. The magnetic susceptibilities of PMNO showed hysteresis between field cooled and zero-field cooled conditions below the transition of 15 K, suggesting that the material has a spin-glass feature. Neutron diffraction patterns of PMNO showed no evidence of a long-range magnetic ordering at 1.5 K, which is consistent with spin-glass behavior. Rietveld refinements of neutron powder diffraction data collected at different temperatures between 1.5 and 700 K have been carried out in order to extract structural information. The crystal structure of this compound is cubic (space group $Pm\bar{3}m$) within the whole temperature interval. The Mn and Nb ions were found to be disordered over the perovskite B-sites. The main feature of this structure is the positional disorder at the Pb site, the importance of which in connection with the ferroic transitions is briefly discussed. The Pb cations show a positional disorder shifting from their high-symmetry positions along the [1 1 1] direction. The effect of Fe-doping on PMNO has been studied. The substitution of Fe at the Mn site in PMFNO results in a small changes of the magnetic properties without significant differences in the crystal structures. The factors governing the observed structural and magnetic properties of PMNO and PMFNO are discussed and compared with those of other quaternary Mn-containing perovskites. For the $\text{PbB}^{3+}_{1/2}\text{Nb}_{1/2}\text{O}_3$ series with the isomorphous substitution B^{3+} , graphs of average lattice parameters of the perovskite phase and the temperatures of ferroelectric and magnetic phase transitions as functions of the B^{3+} cation radius were constructed and are discussed. Influence of A-cation sublattice on magnetic properties is also considered. © 2007 Elsevier Ltd. All rights reserved.

Keywords: A. Electronic materials; C. Neutron scattering; D. Crystal structure; D. Magnetic properties; D. Ferroelectricity

1. Introduction

Materials known as magnetoelectrics, which are simultaneously ferroelectric and ferromagnetic (or at least show some type of magnetic ordering), have recently become the focus of much research [1–4]. These compounds present

* Corresponding author.

E-mail addresses: ivan@cc.nifhi.ac.ru, Sergey.Ivanov@mkem.uu.se (S.A. Ivanov), Per.Nordblad@angstrom.uu.se (P. Nordblad), Roland.Tellgren@mkem.uu.se (R. Tellgren), Hakan.Rundlof@mkem.uu.se (H. Rundlof).

opportunities for a wide range of potential applications [5,6] in addition to that the fundamental physics of multiferroic materials is rich and fascinating [1–4].

The coexistence of ferromagnetism and ferroelectricity is difficult to achieve for many reasons [7] and only very few multiferroic materials are known [8]. First, and most fundamentally, the cations, which are responsible for the electric polarization in conventional ferroelectrics, have a formally empty d-electron configuration. In contrast, ferromagnetism requires unpaired electrons, which in many materials are provided by d electrons of transition metal ions. Therefore the coexistence of the two phenomena, although not prohibited by any physical law or symmetry consideration, is discouraged by the local chemistry that favors one or the other but not both. In practice, alternative mechanisms for introducing the polar ion displacements other than the magnetic transition metal ions, such as stereochemically active lone pairs of Bi^{3+} and Pb^{2+} cations can be used to circumvent this restriction. Because all well-known single-phase multiferroics are mainly Mn- or Fe-based oxides, perovskite oxides containing Bi and Pb cations in the A-sublattice and Mn and Fe cations in the B-sublattice are particularly promising candidates of multiferroic materials.

The capability of perovskite-structured oxides to substitute one ion with another (or a set of ions) without remarkable structural distortion provides a way of obtaining new magnetoelectric perovskites. Studies of the series of complex perovskite-structured oxides, which give insight into the regularities of the structural changes and physical properties (with no allowances for complexity added to the compound composition), are of particular interest. A broad range of ferroelectric and magnetic properties determined by structure peculiarities of the compounds has been investigated in one of the most complete series of isomorphous substitution, $\text{PbB}^{3+}_{1/2}\text{Nb}_{1/2}\text{O}_3$ [9–12] in order to understand the nature of magnetoelectric interactions in these compounds. It is known that the B site can accommodate several kinds of metal ions while the cation arrangement on this sublattice is controlled primarily by the charge difference between the B cations and secondarily by the ionic size difference between them. Depending on the valencies and the ionic radii, the B cations settle either in an orderly or in a random fashion in the lattice. The literature data on the $\text{Pb}(\text{Mn}_{1/2}\text{Nb}_{1/2})\text{O}_3$ are very scarce. The complex perovskite PMNO was first prepared as a ceramic in Refs. [13,14]. However, the specimens obtained were not single-phase, for which reason it was not possible to reliably investigate the properties of the new compound. Later, the synthesis in N_2 atmosphere gave a single-phase ceramic PMNO and it was concluded that this compound was ferroelectric with $T_c = 293$ K and antiferromagnetic below 77 K [15]. No distortion of the perovskite cell in which the two kinds of cations (Mn^{3+} and Nb^{5+}) are randomly distributed at the octahedral B-site positions, was observed at room temperature and the phase was assigned to cubic symmetry (space group $Pm\bar{3}m$) with $a = 4.004$ Å. More extensive studies of the magnetic properties of PMNO was made in [16,17] and the paramagnetic Curie temperature $\Theta = 40$ K was found.

However, numerous discrepant results appeared after single crystals were synthesized [18–20]. In one study it was found a small monoclinic distortion at room temperature ($a \sim b \sim c = 4.006$ Å, $\beta = 90^\circ 5'$). The temperature dependence of the reciprocal magnetic susceptibility obtained in these studies shows anomalies at 135, 73 and 11 K. Below 11 K PMNO was considered as antiferroelectric and antiferromagnetic accompanied by a weak ferromagnetic moment.

A magnetoelectric effect was also found below 11 K [18,19] where the spontaneous magnetic moment could be induced whose magnitude and direction were determined by the magnetic and electric fields imposed on the single crystal during cooling.

The dielectric measurements performed on PbMNO ceramics, do not show the typical broad diffuse phase transition known for Pb-based perovskite relaxors. However, an anomalous increase of the permittivity with clear maximum can be observed at 165 K [15], 400 K [24] and 420 K [16]. The understanding of these anomalies is still a matter of debate and the real magnetic and dielectric properties are much more complicated than originally anticipated.

In the same time, an X-ray study of PMNO single crystal, which was obtained from a high-temperature solution growth [22] showed that the average lattice symmetry is cubic.

In the light of the above considerations, a detailed further characterisation of crystal structure and magnetic properties is still needed.

In the perovskite manganese oxide, the introduction of other transition metal elements, which exhibit dissimilar electronic configuration to Mn, should lead to dramatic effects associated with the electronic configuration mismatch between Mn and the other substituted magnetic ions. In this sense, and in order to avoid the lattice distortion, the Fe atom has been selected regarding the identical ionic radii of Fe^{3+} and Mn^{3+} . At high Fe-doping level, the strong competition between the Mn—O—Mn and the Mn—O—Fe superexchange interactions might also result in spin-glass behavior [23].

The $\text{Pb}(\text{Mn}_{1/4}\text{Fe}_{1/4}\text{Nb}_{1/2})\text{O}_3$ (PMFNO) perovskite was studied only once [24,25], however the structural and magnetic properties have not yet been clarified and the influence of Fe-doping is not clear so far. Mn-doped $(\text{Fe}_{1/2}\text{Nb}_{1/2})\text{O}_3$ (PFNO) ceramic was synthesized [26] and it was shown that small Mn doping (up to 3 mol.%) strongly impair the dielectric properties.

We have studied the structural and magnetic properties of PMNO and PMFNO to determine possible differences in their magnetic properties, arising because of differences between Mn^{3+} (Jahn–Teller ion) and Fe^{3+} ions. In this paper we report the results of X-ray and neutron diffraction studies and magnetic measurements of PMNO and PMFNO, which clearly show the absence of long-range magnetic order and are consistent with a spin-glass (SG) magnetic state. As an important supplement, the $\text{AB}_{1/2}^{3+}\text{Nb}_{1/2}\text{O}_3$ perovskite series ($\text{A} = \text{Ba}, \text{Sr}, \text{Pb}, \text{Ca}$, $\text{B} = \text{Mn}, \text{Fe}, \text{Co}, \text{Ni}, \text{Cr}$) was considered to find the regularities of structure and magnetic properties as a function of the A^{2+} or B^{3+} cation radius.

2. Experimental

Samples of PMNO and PMFNO were prepared by solid-state reaction of inorganic precursor compounds in air, as well as in flowing nitrogen and oxygen. Starting materials were PbO , Nb_2O_5 , Fe_2O_3 and Mn_2O_3 . The reactive powders were mechanically ground and mixed in an agate mortar in an appropriate stoichiometric ratio with 5% excess PbO to prevent loss of lead at elevated temperatures. The mixtures were calcined in a platinum crucible at 1223 K for 4 h. After grinding at room temperature they were annealed for 14 h at 1223 K. The annealing was repeated two times. For synthesis in air the mixtures were quenched to room temperature. The mixtures were heated in flowing N_2 and O_2 to 1223 K with a slope of 10 K/min, annealed for 14 h and slowly cooled to room temperature. In air and O_2 PMNO and PMFNO could be prepared as pure, single-phase perovskites without undesirable stable impurity phases.

The purity of the powder samples was checked from powder X-ray diffraction patterns obtained with a high-resolution SIEMENS D 5000 diffractometer. Filtered $\text{Cu K}\alpha$ radiation ($\lambda = 1.54056 \text{ \AA}$) was used. The diffraction diagram was measured from 10° to 140° in 2θ with step size 0.02° (2θ) and 5 s. counting time per step. Additionally, all reflections were measured with longer, 13 s counting time and shorter, 0.010 step size that allowed for calculation of the lattice parameters. No clear deviation from the cubic symmetry could be observed by XRD.

The chemical composition of the prepared ceramic PMNO and PMFNO samples was analysed by energy-dispersive spectroscopy (EDS) coupled to a transmission electron microscope. The temperature dependence of the magnetization of the samples was measured in a Quantum Design MPMS SQUID magnetometer. Zero-field cooled (ZFC) and field cooled (FC) protocols were used. The ZFC measurements were performed by cooling the PMNO and PMFNO samples down to 5 K, applying the field and measuring the magnetization when the sample was heated. The sample was then cooled back to 5 K in the applied field and the FC magnetization measured on reheating the sample without changing the magnetic field.

EPR experiments were performed at 9.46 GHz using a Bruker (ER-200D) reflection X-band type spectrometer. The spectrum was measured at room temperature by sweeping magnetic field from 0 to 6000 Oe.

Because the neutron scattering lengths of Mn, Fe and Nb are strongly different, the chemical composition of the B-site cations can be observed by neutron powder diffraction (NPD) with good precision ($b_{\text{Mn}} = -3.75$, $b_{\text{Fe}} = 9.45$, $b_{\text{Nb}} = 7.05 \text{ fm}$). The neutron scattering length of oxygen ($b_{\text{O}} = 5.80 \text{ fm}$) is comparable to those of the heavy atoms and NPD provide an accurate information on its position and stoichiometry. Neutron diffraction study was carried out on these materials using the powder diffractometer at the R2 reactor in Studsvik, Sweden and the G4.1 diffractometer at LLB, Saclay, France. Two different wavelengths were employed to investigate the possibility of magnetic ordering (2.4255 \AA , Saclay) and to obtain an accurate structural refinement (1.470 \AA , Studsvik). NPD patterns were registered at different temperatures (10–700 K). Corrections for absorption effects were subsequently carried out in the Rietveld refinements, utilizing an empirical value of μR . Structural refinements were performed by the Rietveld method, using the FULLPROF software [27]. The diffraction peaks were described by a pseudo-Voigt profile function, with a Lorentzian contribution to the Gaussian peak shape. A peak asymmetry correction was made for angles below 35° in 2θ . Background intensities were described by a polynomial with six coefficients. The ideal cubic perovskite structure (space group $Pm\bar{3}m$), where all atoms are fixed at special positions, was taken as a starting model for the Rietveld refinements.

3. Results

According to the elemental analyses done on 20 different crystallites, the metal composition of PMNO is $\text{Pb}_{0.97(4)}\text{Mn}_{0.52(3)}\text{Nb}_{0.51(3)}$, and PMFNO is $\text{Pb}_{0.98(4)}\text{Mn}_{0.26(3)}\text{Fe}_{0.23(3)}\text{Nb}_{0.53(3)}$ if the sum of the cations is assumed to be 2. The microstructure of the obtained powders, observed by scanning electron microscopy, reveals uniform and fine grain distribution. The first crystallographic characterization of the samples was performed by X-ray powder diffraction analysis at room temperature, which showed that the prepared samples of PMNO and PMFNO formed a single-phase powder. The room temperature XRD pattern of PMNO could be indexed on the basis of a primitive cubic unit cell with $a = 4.0085(1)$ Å, thus without ordering of the Mn and Nb ions on the octahedral sites. This value is in good agreement with the lattice parameter obtained from single crystal data ($a = 4.004(2)$ Å) [18]. There is, however, a slight disagreement with the cell parameters of the ceramic samples reported in Refs. [28] and [29], where $a = 4.012$ and 4.015 Å, respectively, the difference in lattice parameters could be explained by comparing the two different synthesis methods.

The X-ray diffractograms of PMNO and PMFNO are very similar (Fe^{3+} and Mn^{3+} cations have the same size) and the powder pattern of PMFNO could be indexed to a cubic lattice with lattice constant $a = 4.0131(1)$. X-ray diffraction patterns were recorded for PMNO and PMFNO at different temperatures (90–700 K). Within the whole temperature range the samples remain single-phase and show cubic symmetry. In our XRD and NPD data, it was impossible to find a monoclinic distortion as proposed in [21].

It can be found that PMNO and PMFNO samples show some common features in the EPR behavior: the spectrum consists of a single broad Lorentzian line without any structure and the resonance field corresponds to a constant g -value very close to 2. This observed g -value is in agreement with the reported value of g obtained for Fe^{3+} and Mn^{3+} cations. The detailed analysis of EPR spectra will be presented elsewhere.

Fig. 1 shows zero-field cooled and field cooled magnetization curves measured on PMNO in a magnetic field of 20 Oe. The main frame includes a major temperature range 5–300 K, and the inset the results from measurements confined to the range 5–35 K. The ZFC and FC curves merge just above the temperature of a pronounced maximum in the ZFC curve. The behavior above this temperature does not follow a Curie–Weiss law, a plot of $1/M$ versus T yields a curve with steadily increasing slope that at high temperatures (>150 K) levels out towards a straight line. A linear fit of the high-temperature data gives a Weiss temperature of about 70 K. The low-temperature behavior indicates a spin-glass transition—looking at the inset of Fig. 1, there is a cusp in the ZFC curve at 15 K indicating a freezing temperature, T_f , a rather flat FC curve at temperatures below this temperature and the ZFC and FC curves merge above the temperature T_f . It is worth to notice an additional weak but rather sharp onset of irreversibility between the ZFC and FC that appears at about 65 K when the temperature range is extended to higher temperatures as in the main frame of Fig. 1. This faint anomaly does not originate from the main phase of the sample, but must have its origin in a magnetic phase transition in an impurity phase of an amount far below the detection limit of XRD and NPD experiments.

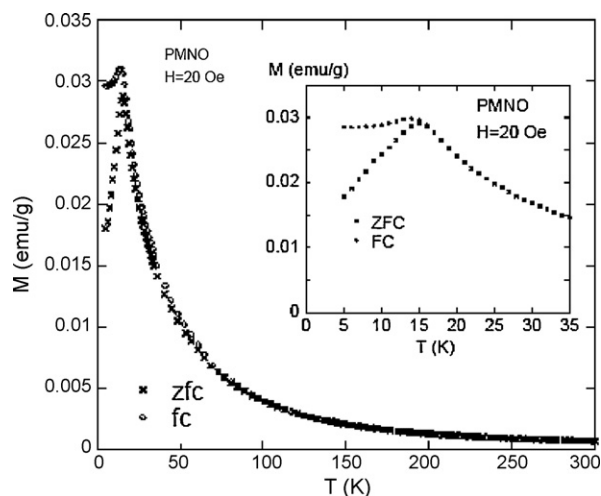


Fig. 1. Temperature dependence of the magnetization of $\text{Pb}(\text{Mn}_{1/2}\text{Nb}_{1/2})\text{O}_3$ ($H = 20$ Oe).

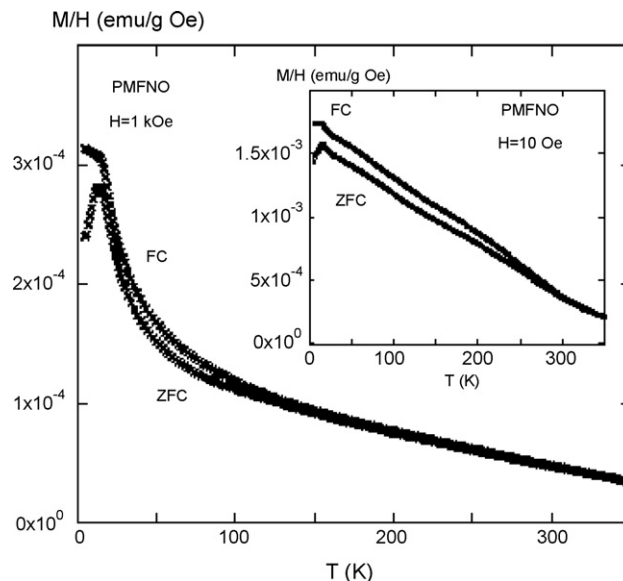


Fig. 2. Temperature variation of ZFC and FC susceptibility curves in an external fields 10 Oe and 1 kOe of $\text{Pb}(\text{Mn}_{1/4}\text{Fe}_{1/4}\text{Nb}_{1/2})\text{O}_3$.

The PMFNO sample has an apparently more complicated behavior; Fig. 2 shows ZFC and FC ‘susceptibility’ (M/H) curves measured in 10 (inset) and 1000 Oe (main frame) applied fields. There is a strong suppression of the M/H values at all temperatures indicating nonlinear magnetization response. The non-linearity is most probably due to a minor ferro- (or ferri-) magnetic impurity phase, the amount of which is lower than can be resolved in neutron or X-ray diffraction. This conclusion is also supported by the strong field dependence of the temperature for a first bifurcation of the ZFC and FC curves, which occurs at about 270 K in 10 Oe and around 130 K in 1000 Oe field. Assuming that the contribution from this phase is almost saturated at 1000 Oe, one can derive a spontaneous moment of this phase that is smaller than 0.1 emu/g. (If the impurity is assumed to be Fe_3O_4 : it amounts to less than 0.2% of the total mass). It is only at lower temperatures that the contribution from the main phase yields a significant (10 Oe) or dominant (1000 Oe) contribution to the temperature dependence of the M/H versus T curves. At low temperatures there is a rather sharp maximum in the ZFC curve at 15 K and a flattening out of the FC curve below this temperature. The ZFC maximum becomes broader with increasing field. This behavior is as in the case of PMNO characteristic of spin-glass behavior.

The cusp-like feature and divergence in the FC/ZFC susceptibility is a tell-tale sign of a spin-glass transition [30–32], yet these features have also been seen in samples that exhibit long-range magnetic ordering. Even though the magnetic sublattice is highly frustrated, such an ordering is always possible, and to investigate this series of low-temperature neutron scattering experiments are needed.

As a starting model for the Rietveld refinement of our NPD data sets for PMNO and PMFNO, the ideal cubic perovskite structure (space group $Pm\bar{3}m$) was taken with the atoms fixed at their special Wyckoff positions, namely (1a), (1b) and (3c), for Mn/Nb or Mn/Fe/Nb, Pb and O, respectively. During our refinement the relative concentrations of the B-site cations were constrained to the overall bulk stoichiometry but the fraction of Mn cation in PMNO was allowed to vary. The concentration ratio Mn/Nb was refined to a value of 1 and the oxygen concentration to a value close to 1.00 (in the frames of 2 standard deviations) and no evidence was found for a partial occupancy of the oxygen site. No extra peaks or additional splittings of the main reflections were observed, which would indicate the need for symmetry lower than cubic.

Refinement of the crystal structure at 700 K (in paraelectric and paramagnetic phases) led to a very large temperature factor for the Pb cations ($B_{\text{Pb}} = 4.21(7) \text{ \AA}^2$ and $4.35(7) \text{ \AA}^2$ for PMNO and PMFNO, respectively) in agreement with findings on other lead-containing perovskites [33–37]. It is most likely that the large B -values can be attributed to some static or dynamic structural disorder and that the Pb cation is locally displaced from its ideal position. The correlation length of these shifts is relatively short and, thus this effect is incorporated into the displacement parameter during the Rietveld refinements. Pb is seldom found at its idealised special position, but rather

statistically distributed over several sites around it. Since the off-centering of Pb provides strong dipolar moment, the direction of the Pb off-centering is of great importance. Lone-pair electrons in Pb results in formation of the short Pb—O bonds, giving rise to strong Pb polarizability. In average Pb atom is off-centered against the O_{12} cage by as much as 0.2 Å. Such a deformation will produce local polarization.

In the next stage of our refinements, the structural models including the $[1\ 0\ 0]$, $[1\ 1\ 0]$ and $[1\ 1\ 1]$ disorders on the Pb atom were examined by the Rietveld refinement adopting the split-atom method, where one Pb atom is assumed to randomly occupy the six $(x\ 0\ 0)$, the twelve $(x\ x\ 0)$ and the eight $(x\ x\ x)$ equivalent sites, respectively, around the $(0\ 0\ 0)$ position. The value of the R_B factor was plotted as a function of different Pb displacements. During the refinements only the thermal parameter B_{Pb} was varied. All three structural models refined successfully, leading to significant reductions in the thermal parameters of the Pb cations. The best numerical improvement of the R_B -factor was obtained for the model in which the Pb ions statistically occupies the (8 g) position, which correspond to a shift along the $[1\ 1\ 1]$ directions from the ideal (1b) position by a distance of 0.15–0.17 Å (see Fig. 3). In this case the temperature factor, B_{Pb} , recovers a normal value (for 700 K) and a clear minimum of the agreement factor was found (see Table 1). The same type of refinements was performed at different temperatures. The temperature evolution of Pb displacement for PMnO and PMFNO is presented on Fig. 4. The Mn and Nb cations are distributed randomly at the B-site of PMNO and the size of the oxygen octahedron surrounding Mn should in principle be different in size compared to the octahedron containing Nb. Several attempts have been performed to separate Mn and Nb cations constraining their thermal parameters during the refinements. When B-site cation positions in PMNO were allowed to refine separately, the refinement was unstable and without improvement in the fit.

The possibility of Mn/Fe/Nb and O disorders from their special Wyckoff positions was also examined, but the R-factors and the fitting feature were not significantly improved by the Rietveld refinement. These atoms were left at their special sites after verifications that their displacements did not improve the refinement. The oxygen anions were also

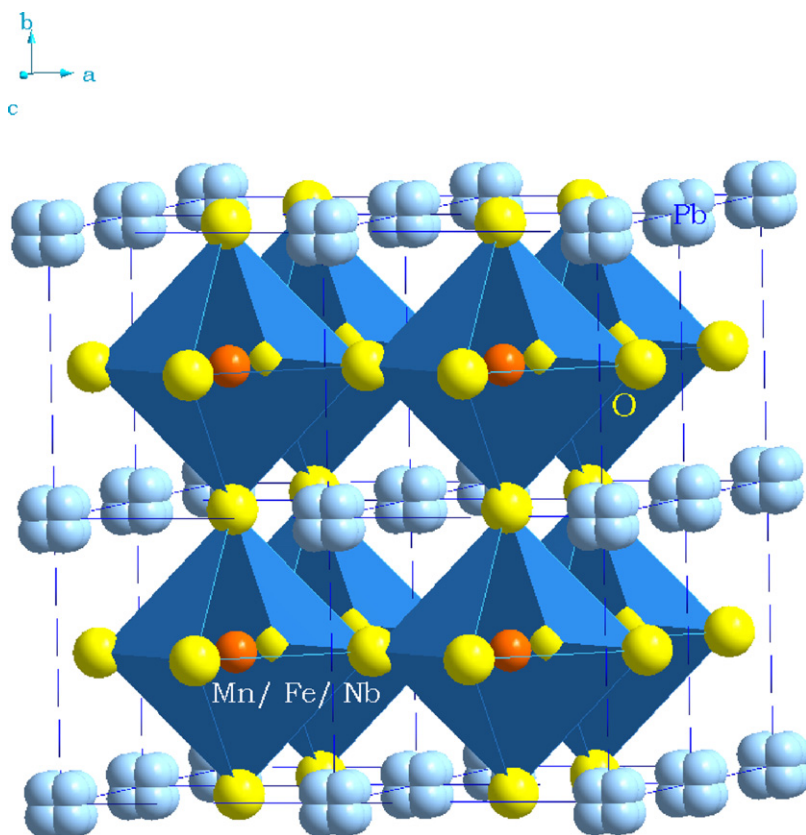


Fig. 3. A polyhedral view of the cubic perovskite structure of $Pb(Mn_{1/4}Fe_{1/4}Nb_{1/2})O_3$ at room temperature. The Pb atom is disordered at multisites in $[1\ 1\ 1]$ directions from the $(0\ 0\ 0)$ position of the ideal cubic structure.

Table 1

Isotropic thermal displacement parameter of Pb (B_{Pb}), off-center magnitude (δ_{Pb}) of Pb atom, reliability factors obtained by Rietveld refinement of PMNO at 700 K, assuming both order and disorder models of Pb atom in the [1 0 0], [1 1 0] and [1 1 1] directions

Model	Order model	Disorder model		
		[1 0 0]	[1 1 0]	[1 1 1]
B_{Pb} (\AA^2)	4.21(7)	2.23(6)	1.98(6)	1.77(6)
δ_{Pb}		0.058(1)	0.048(1)	0.039(1)
R_{p} (%)	3.71	3.52	3.23	3.16
R_{wp} (%)	4.69	4.48	4.29	4.21
R_{B} (%)	6.95	5.38	4.86	4.59

The lowest R -values are indicated in bold.

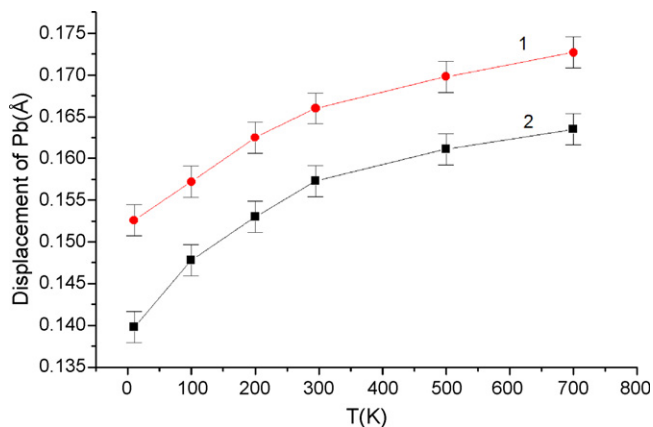


Fig. 4. Temperature dependence of Pb cation displacements in $\text{Pb}(\text{Mn}_{1/4}\text{Fe}_{1/4}\text{Nb}_{1/2})\text{O}_3$ (1) and $\text{Pb}(\text{Mn}_{1/2}\text{Nb}_{1/2})\text{O}_3$ (2).

refined individually with free occupancy parameters that did not improve the final fit. Thus, the oxygen positions were set to be fully occupied in the final refinement. Refinements with anisotropic temperature factors assigned to oxygen gave an improved fit with the mean-square displacements corresponding to vibrations mainly within the faces of a primitive cubic cell. This disk-shaped thermal ellipsoid of oxygen anions points out some dynamic and/or static displacements within the face of the cube.

From individual Pb—O, Mn—O and Nb—O distances the valences of the cations were calculated following the phenomenological Brown's Bond-Valence Model (BVS) proposed in [38]. Pb and Mn cations exhibit valences +1.96(1) and +3.12(1), respectively, which is slightly different from those expected in this compound, of +2 and +3. The valence of the Nb cation is somewhat lower than +5 (+4.82(1)).

Tables 2 and 3 list the structural parameters for PMNO and PMFNO, respectively: atomic coordinates, lattice parameters, thermal displacement parameters, as well as the reliability factors.

The observed, calculated and difference plots of PMNO and PMFNO at 700 and 10 K are shown in Figs. 5 and 6, respectively. From the sequential data collection, the temperature evolution of the lattice parameter has been studied (see Fig. 7). It is very important because it gives us the temperature dependence of the Mn/Nb—O interatomic distance ($a = d(\text{Mn/Nb—O}) \times 2$). At low temperatures the thermal expansion of PMNO and PMFNO is close to zero and remains practically unaltered up to approximately 300 K. This phenomenon is common along the complex Pb-based relaxor perovskites and can be associated with the electrostriction effect [27]. The thermal expansion of relaxors is composed of electrostrictive and thermal components, with the electrostrictive component being negative within a certain temperature range where the diffuse phase transition occurs. The cumulative effect of the two contributions to the total thermal expansion may be near zero or even negative. Although the temperature dependence of the lattice parameters across the ferroelectric phase transition ($T_c = 400\text{--}420$ K [16,21,24]) do not apparently show abrupt discontinuity, a change in its slope can be attributed to this phase transformation. Above the supposed ferroelectric phase transition, the evolution of the lattice parameter exhibits a typical linear expansion with the increase in temperature. However, additional experimental studies with small temperature step are required in order to make this clearer.

Table 2
Comparison of Rietveld refinement results of PMNO for different temperatures (space group $Pm\bar{3}m$)

T (K)		10	295	700
a (Å)		4.0068(2)	4.0087(3)	4.0310(4)
Pb	x	0	0	0
	y	0	0	0
	z	0	0	0
	B (Å ²)	3.19(6)	3.33(7)	4.21(7)
	Pb—O (Å)	2.83(1)	2.83(1)	2.85(1)
	x	0.035(1)	0.039(2)	0.040(3)
	y	0.035(1)	0.039(2)	0.040(3)
	z	0.035(1)	0.039(2)	0.040(3)
	B (Å ²)	0.97(3)	1.21(4)	1.77(6)
	Pb—O, Å x3	3.03(1)	3.06(1)	3.08(1)
Mn/Nb	x6	2.84(1)	2.85(1)	2.86(1)
	x3	2.64(1)	2.62(1)	2.63(1)
	x	1/2	1/2	1/2
	y	1/2	1/2	1/2
	z	1/2	1/2	1/2
	B (Å ²)	0.23(2)	0.57(3)	0.86(4)
O	Mn/Nb—O (Å)	2.00(1)	2.00(1)	2.02(1)
	x	1/2	1/2	1/2
	y	1/2	1/2	1/2
	z	0	0	0
	B (Å ²)	0.87(3)	1.26(4)	1.61(6)
	$B_{11} \times 10^4$ (Å ²)	264(9)	281(10)	436(15)
	$B_{33} \times 10^4$ (Å ²)	153(10)	136(13)	181(18)
R_{po} (%); R_{pd} (%)		3.38; 2.98	3.47; 3.09	3.71; 3.16
R_{wpo} (%); R_{wpd} (%)		4.18; 3.83	4.25; 3.88	4.69; 4.21
R_{Bo} (%); R_{Bd} (%)		5.54; 4.41	5.69; 4.17	6.95; 4.59
χ_o^2 ; χ_d^2		1.65; 1.56	1.62; 1.54	1.68; 1.53

Indexes used to distinguish R -factors of different models: “o” for ordered model and “d” for disordered model.

Neutron diffraction data collected between 1.5 and 295 K for PMNO and PMFNO are presented in Figs. 8 and 9, respectively. Additional maxima in the 1.5 K neutron diffraction data, expected for a three-dimensionally ordered antiferromagnetic state below 15 K in PMNO and PMFNO were not present, indicating that a long-range magnetically ordered state is not achieved. This feature points directly to a freezing of the spins below a temperature close to 15 K, i.e. spin-glass behavior.

4. Discussion

The Mn and Nb cations are apparently disordered over the octahedral sites of the perovskite structure with half of the sites occupied by a magnetic cation. With such a high concentration of magnetic species, well above the percolation limit, it is entirely reasonable for the compound to order antiferromagnetically at low temperatures. We would expect the superexchange along a pathway Mn—O—Mn to be the strongest magnetic interaction in such a system, and that a G-type magnetic structure would be adopted. However, the behavior of the FC and ZFC susceptibilities and the absence of magnetic scattering from the low-temperature diffraction pattern all indicate that this is not the case. The absence of magnetic Bragg peaks proves that there is no long-range magnetic ordering. We therefore conclude that we are dealing with a spin-glass, and this conclusion is supported by the magnetic susceptibility data.

Unusually large atomic displacement factor associated with the Pb sites provide strong evidence for disordered atomic shifts in PMNO and PMFNO. Furthermore, a reduction in temperature leaves this disorder unaltered. This phenomenon is likely to be due to the electronic configuration of the Pb²⁺ cation.

The temperature of the magnetic phase transition (T_M) for A(Mn_{1/2}Nb_{1/2})O₃ (A = Ba, Pb, Sr, Ca) [9–11,39,40] is the same order (see Fig. 10). It shows a relatively weak linear decrease in T_M versus the size of the A-site cation. This is

Table 3
Comparison of Rietveld refinement results of PMFNO for different temperatures (space group $Pm\bar{3}m$)

T (K)		10	295	700
a (Å)		4.0126(3)	4.0131(3)	4.0308(4)
Pb	x	0	0	0
	y	0	0	0
	z	0	0	0
	B (Å ²)	3.33(7)	3.24(7)	4.13(9)
	Pb—O (Å)	2.83(1)	2.84(1)	2.85(1)
	x	0.038(1)	0.041(2)	0.042(3)
	y	0.038(1)	0.041(2)	0.042(3)
	z	0.038(1)	0.041(2)	0.042(3)
	B (Å ²)	2.89(5)	3.07(6)	4.13(6)
	Pb—O, Å $\times 3$	3.06(1)	3.08(1)	3.10(1)
Mn/Fe/Nb	x_6	2.85(1)	2.85(1)	2.87(1)
	x_3	2.63(1)	2.61(1)	2.62(1)
	x	1/2	1/2	1/2
	y	1/2	1/2	1/2
	z	1/2	1/2	1/2
	B (Å ²)	0.19(2)	0.51(3)	0.79(4)
O	Mn/Fe/Nb—O (Å)	2.00(1)	2.01(1)	2.02(1)
	x	1/2	1/2	1/2
	y	1/2	1/2	1/2
	z	0	0	0
	B (Å ²)	0.81(3)	1.22(4)	1.57(6)
	$B_{11} \times 10^4$ (Å ²)	251(9)	273(10)	424(14)
	$B_{33} \times 10^4$ (Å ²)	135(10)	141(14)	160(17)
R_{po} (%); R_{pd} (%)	3.64; 3.11	3.76; 3.23	4.14; 3.65	
R_{wpo} (%); R_{wpd} (%)	4.26; 3.92	4.35; 3.97	5.18; 4.67	
R_{Bo} (%); R_{Bd} (%)	5.59; 4.17	5.87; 4.49	6.71; 5.28	
χ_o^2 ; χ_d^2	2.08; 2.14	1.99; 2.19	2.16; 2.07	

Indexes used to distinguish R -factors of different models: “o” for ordered model and “d” for disorder model.

in agreement with the band structure calculations of Nb-based perovskites where the substitution in the A site does not change the band gap significantly [41].

The understanding of this effect will require a deeper investigation.

For comparative analysis of the structural features of the $AMn_{1/2}^{3+}Nb_{1/2}O_3$ compounds adopting the cubic perovskite structure, the average lattice parameter of the unit cell (uc) $a = (V_{uc})^{-1/3}$ was plotted as a function of the A^{2+} -cation radius (Fig. 11) (the values of ionic radii were employed with regard to the coordination number). As seen from this Fig. 11, there is practically linear dependence a versus R_A .

Using the data available on dielectric (T_{CE}) and magnetic (T_{CM}) phase transitions of the $PbB_{1/2}^{3+}Nb_{1/2}O_3$ perovskite compound series ($B = Mn, Fe, Co, Ni, Cr$) [9–11,39,40,42] including our data for PMNO we have plotted the dependence of these temperatures on the B^{3+} -cation radius (Fig. 12). The figure shows two different dependences which support the conclusion, that the coexistence of ferroelectricity and magnetism is discouraged by the local chemistry that favors one or the other but not both [8]. The characteristic feature of the $PbB_{1/2}^{3+}Nb_{1/2}O_3$ perovskite series is based on the fact that all presented perovskites are always disordered.

It should, however, be particularly emphasized that this analysis involves difficulties arising from the fact that the available structural and physico-chemical data are very restricted.

Consequently, it is difficult to find a simple explanation for the different values of T_{CE} and T_{CM} based on only crystallo-chemical considerations using the tolerance factor (t), the lattice parameter (a) and the volume (V) of the unit cell. It is necessary to carry out detailed structural investigations of complex metal oxides with different B-site cations in order to clarify the possible correlations between the structure, magnetic and dielectric properties. It is, however, clear that the decrease of the lattice parameter a in this type of cubic perovskite structure (which is equivalent of decreasing the Mn—Mn distance) could result in the increase of T_{CM} . This simple rule holds for the compared Pb-

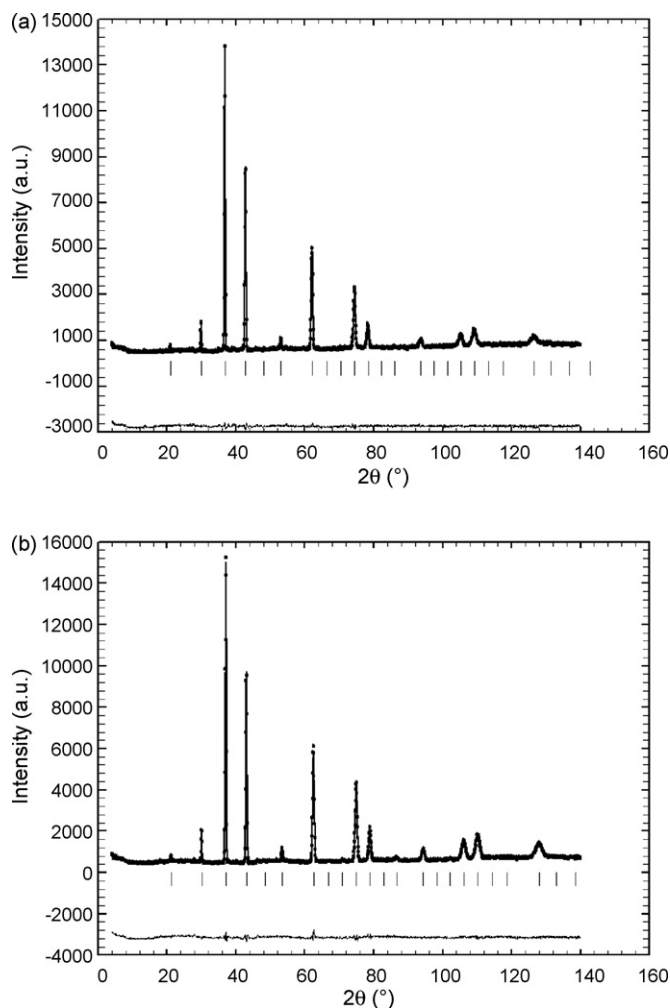


Fig. 5. The observed, calculated, and difference plots for the fit to NPD patterns of $\text{Pb}(\text{Mn}_{1/2}\text{Nb}_{1/2})\text{O}_3$ after Rietveld refinement of the nuclear and magnetic structure at different temperatures: 700 K (a) and 10 K (b).

containing perovskite compounds. It is also evident that the off-center polar distortion, which is created, by the Pb and O atoms is responsible for the ferroelectricity. At the same time the magnetic properties strongly depend on the B-site ordering and on the relative concentration of the magnetic cation. With a decrease of the Mn content in the B-perovskite sublattice will follow a progressive decrease of the magnetic properties, which is vividly illustrated for $\text{Pb}(\text{Mn}_{1/4}\text{Mg}_{1/4}\text{Nb}_{1/2})\text{O}_3$ [15].

As a final remark, PMNO and PFNO compounds belong to the perovskite family where some kind of ferroelectricity and magnetism can coexist. For both compounds magnetic (Fe or Mn) and nonmagnetic (Nb) cations share the B-site randomly. But some differences between PMNO and PFNO are evident in spite of the same size of Mn^{3+} and Fe^{3+} cations:

- PMNO adopts a cubic structure in a wide temperature range (1.5–700 K), while PFNO has shown a sequence of symmetry changes from cubic to monoclinic [43];
- PFNO undergoes a long-range antiferromagnetic transition at 143–170 K and spin-glass behavior below 9 K [44], in the case PMNO a spin-glass state is the only one observed magnetic phenomenon;
- The $\text{Fe}^{3+}\text{—O—Fe}^{3+}$ interactions should be antiferromagnetic, but a Jahn–Teller cation like Mn^{3+} demonstrates the $\text{Mn}^{3+}\text{—O—Mn}^{3+}$ ferromagnetic interactions [45].

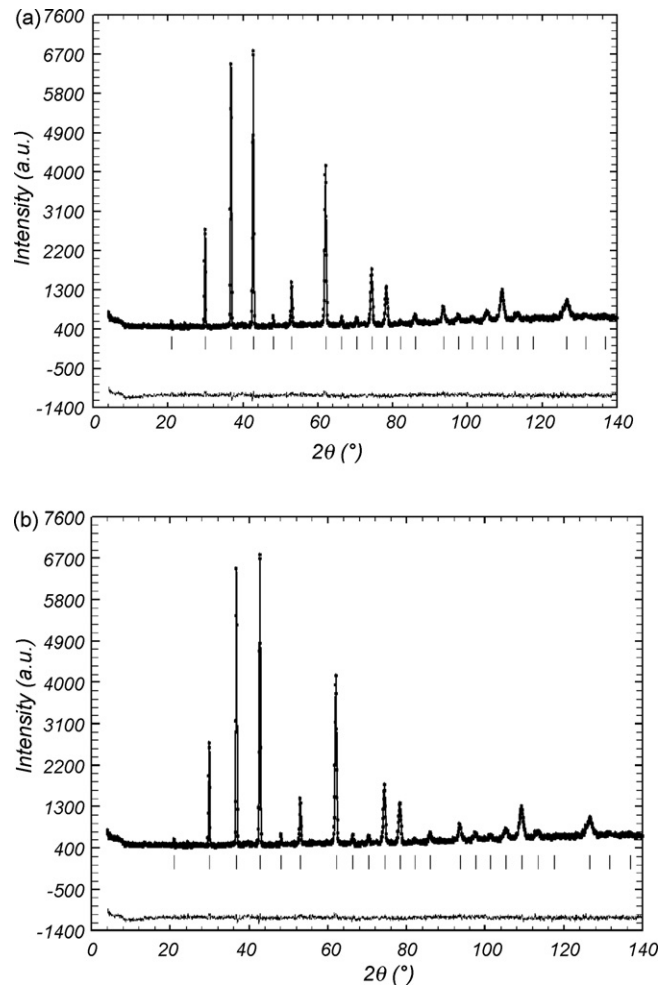


Fig. 6. The observed, calculated, and difference plots for the fit to NPD patterns of $\text{Pb}(\text{Mn}_{1/4}\text{Fe}_{1/4}\text{Nb}_{1/2})\text{O}_3$ after Rietveld refinement of the nuclear and magnetic structure at different temperatures: 700 K (a) and 10 K (b).

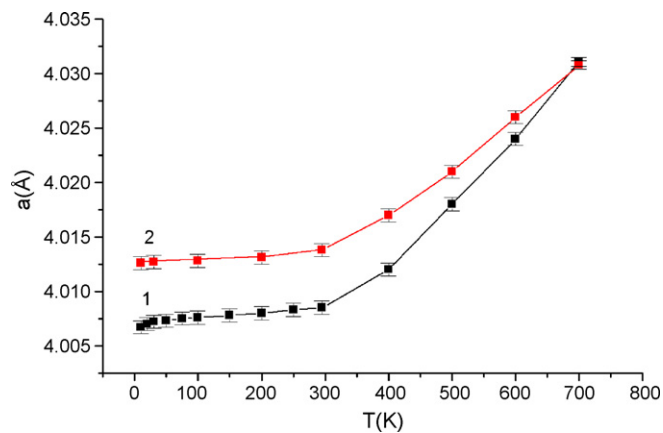


Fig. 7. Temperature dependence of the lattice parameter of $\text{Pb}(\text{Mn}_{1/2}\text{Nb}_{1/2})\text{O}_3$ (1) and $\text{Pb}(\text{Mn}_{1/4}\text{Fe}_{1/4}\text{Nb}_{1/2})\text{O}_3$ (2).

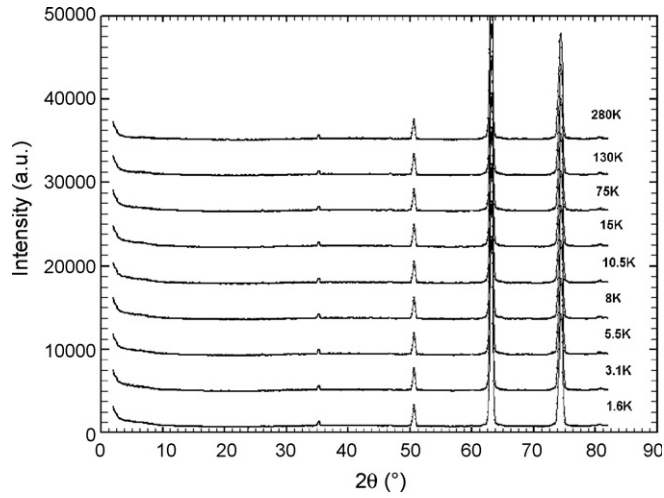


Fig. 8. Temperature evolution of the NPD patterns of $\text{Pb}(\text{Mn}_{1/2}\text{Nb}_{1/2})\text{O}_3$.

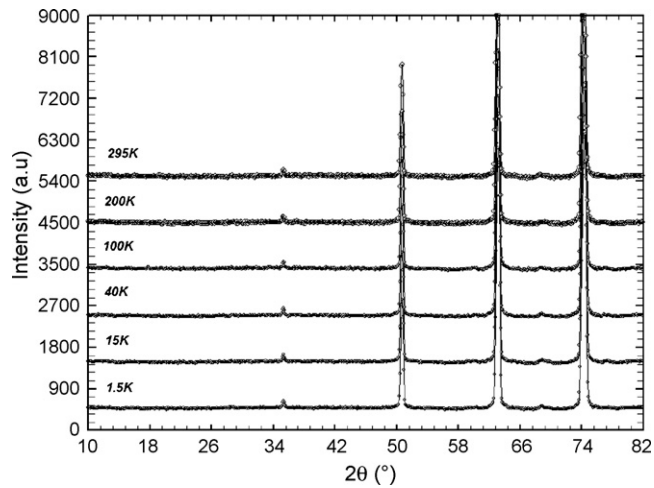


Fig. 9. Temperature evolution of the NPD patterns of $\text{Pb}(\text{Mn}_{1/4}\text{Fe}_{1/4}\text{Nb}_{1/2})\text{O}_3$.

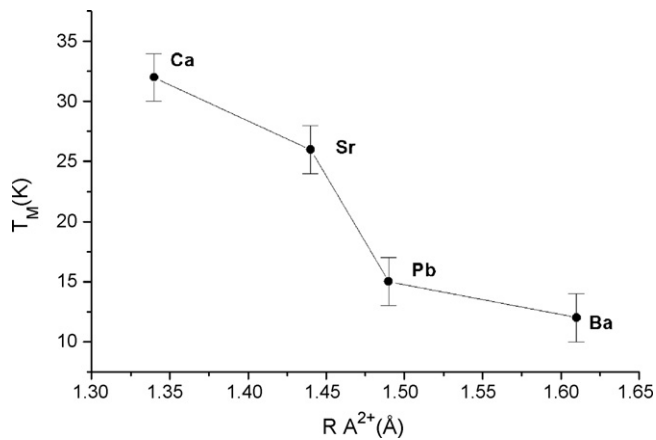


Fig. 10. Variation of the magnetic phase transition temperature for ferroelectric perovskite compounds of $\text{A}^{2+}\text{Mn}_{1/2}{}^{3+}\text{Nb}_{1/2}\text{O}_3$ ($\text{A} = \text{Ba}, \text{Sr}, \text{Pb}, \text{Ca}$) with A^{2+} -cation radius.

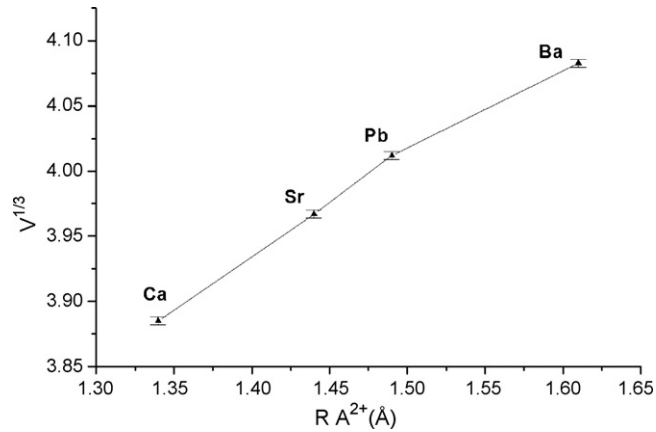


Fig. 11. Average lattice parameter as a function of the A^{2+} -cation radius for the perovskite phases of $A^{2+}Mn_{1/2}{}^{3+}Nb_{1/2}O_3$ ($A = Ba, Sr, Pb, Ca$).

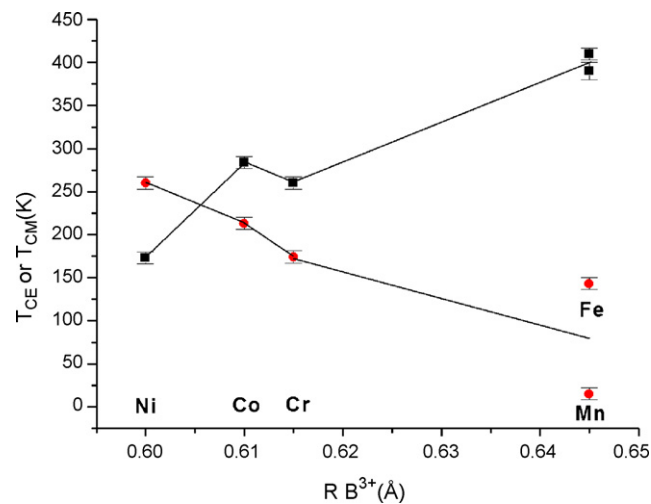


Fig. 12. Variation of ferroelectric (T_{CE}) (circle) and magnetic (T_{CM}) (square) phase transition temperatures for perovskite compounds of $PbB_{1/2}{}^{3+}Nb_{1/2}O_3$ with B^{3+} -cation radius.

Finally, looking at the results given above the different magnetic properties of PMNO and PFNO can be explained in terms of interactions between a disordered array of magnetic Fe^{3+} or Mn^{3+} cations on the B-site when a super-exchange interaction is favored instead of double-exchange interactions. But the rightfulness of this mechanism is still under discussion and more additional experimental data are needed before we can be confident about this explanation.

5. Conclusions

The most remarkable result of this research consists of a new interpretation of the structural and magnetic behavior of the PMNO and PMFNO. The compounds show several similar physical features due to the same long-range disordered perovskite structure. All the results point out that the magnetic anomaly at 15 K, observed by some authors in the past, can be ascribed to a spin-glass transition. The cubic structures of PMNO and PMFNO are characterized by a high degree of Pb positional disorder, which appears to be present over a wide range of temperature. Its displacements with respect to the ideal position is near the same as in other similar $PbB_{1/2}{}^{3+}Nb_{1/2}O_3$ perovskites, for example $PbFe_{1/2}Nb_{1/2}O_3$ [37] and $PbSc_{1/2}Nb_{1/2}O_3$ [46]. At low temperature this Pb disorder remains large and appears to remain even at 10 K. Different magnetic properties of PMNO and PFNO can be explained in terms of interactions

between a disordered array of magnetic Fe^{3+} or Mn^{3+} cations on the B-site where instead of double-exchange interactions, super-exchange interactions are favored.

Acknowledgement

Financial support of this research from the Royal Swedish Academy of Sciences and the Russian Foundation for Basic Research (grant 06-03-32449) is gratefully acknowledged.

References

- [1] D.I. Khomskii, *J. Magn. Magn. Mater.* 306 (2006) 1.
- [2] J.F. Scott, *Nat. Mater.* 6 (256) (2007).
- [3] W. Eerenstein, N.D. Mathur, J.F. Scott, *Nature* 442 (2006) 759.
- [4] W. Prellier, M.P. Singh, P.J. Murugavel, *J. Phys.: Condens. Matter* 17 (2005) R803.
- [5] M. Fiebig, *J. Phys. D: Appl. Phys.* 38 (2005) R123.
- [6] A.J. Freeman, H. Schmid (Eds.), *Magnetoelectric Interaction Phenomena in Crystals*, Gordon and Breach, London, 1995.
- [7] N.A. Hill, A. Filippetti, *J. Magn. Magn. Mater.* 242 (2002) 976.
- [8] N.A. Hill, *J. Phys. Chem. B* 104 (2000) 6694.
- [9] G.A. Smolenskii, V.A. Bokov, V.A. Isupov, *Physics of Ferroelectric Phenomena*, Nauka, Leningrad, 1987.
- [10] Y.N. Venetsev, V.V. Gagulin, V.N. Lyubimov, *Ferroelectromagnets*, Nauka, Moscow, 1982.
- [11] Y.N. Venetsev, E.D. Politova, S.A. Ivanov, *Ferro- and Antiferroelectrics of Barium Titanate Family*, Chemistry Publ, Moscow, 1985.
- [12] V.A. Isupov, *Izv Akad Nauk SSSR Ser. Fiz* 47 (1983) 559.
- [13] G.A. Smolenskii, A.I. Agranovskaya, V.A. Isupov, *Sov. Phys. Solid State* 1 (1959) 1429.
- [14] V.S. Filipiev, M.T. Kupriyanov, E.G. Fesenko, *Sov. Phys. Crystallogr.* 8 (1969) 630.
- [15] Y.E. Roginskaya, Y.N. Venetsev, G.S. Zhdanov, *Sov. Phys. JETP* 21 (1965) 817.
- [16] E.E. Havinga, *Philips Res. Rep.* 21 (1966) 49.
- [17] E.E. Havinga, *ibid.* 21 (1966) 432.
- [18] L.A. Drobyshev, B.I. Alshin, Y.Y. Tomashpolski, Y.N. Venetsev, *Sov. Phys. Crystallogr.* 14 (634) (1970).
- [19] D.N. Astrov, B.I. Alshin, Y.Y. Tomashpolski, Y.N. Venetsev, *Sov. Phys. JETP* 28 (1969) 1123.
- [20] R.V. Zorin, B.I. Alshin, D.N. Astrov, *Sov. Phys. Solid State* 13 (1969) 2862.
- [21] D.N. Astrov, B.I. Alshin, R.V. Zorin, L.A. Drobyshev, *Sov. Phys. JETP* 28 (1969) 1123.
- [22] I.H. Brunskill, R. Bouteller, W. Depmeier, H. Schmid, *J. Cryst. Growth* 56 (1982) 541.
- [23] J.J. Blanco, M. Insausti, I. Gil de Muro, L. Lezama, T. Rojo, *J. Solid State Chem.* 179 (2006) 623.
- [24] J. Modlich, O. Jarchow, T. Rentschler, A. Reller, U. Bismayer, *Solid State Ionics* 95 (1997) 131.
- [25] S. Sharma, P. Choudhary, R. Sati, *J. Mater. Sci. Lett.* 12 (1993) 530.
- [26] B. Fang, Y. Shan, H. Imoto, *Jpn. J. Appl. Phys.* 43A (2004) 2568.
- [27] J. Rodrigues-Carvajal, *Physica B* 192 (1993) 55.
- [28] E.G. Fesenko, M.F. Kupriyanov, R.U. Devlikanova, V.S. Filipiev, *Sov. Phys. Crystallogr.* 19 (1974) 67.
- [29] S.S. Lopatin, T.G. Lupeiko, T.I. Ivleva, *Inorg. Mater.* 23 (1987) 558.
- [30] K. Binder, A.P. Young, *Rev. Mod. Phys.* 58 (1986) 801.
- [31] D. Chowdhury, *Spin Glasses and Other Frustrated Systems*, World Scientific Publishing, Singapore, 1986.
- [32] P.A. Young (Ed.), *Spin Glasses and Random Fields*, World Scientific, Singapore, 1997.
- [33] S.A. Ivanov, S.G. Eriksson, R. Tellgren, H. Rundlof, *Mater. Res. Bull.* 39 (2004) 2317.
- [34] S.A. Ivanov, R. Tellgren, H. Rundlof, N.A. Thomas, S. Ananta, *J. Phys.: Condens. Matter* 12 (2000) 2393.
- [35] N.W. Thomas, S.A. Ivanov, S. Ananta, R. Tellgren, H. Rundlof, *J. Eur. Ceram. Soc.* 9 (1999) 2667.
- [36] A. Geddo Lehmann, F. Kubel, H. Schmid, *J. Phys.:Condens. Matter* 9 (1997) 8201.
- [37] N. Lampis, P. Sciau, A. Geddo-Lehmann, *J. Phys.:Condens. Matter* 11 (1999) 3489.
- [38] N.E. Brese, M. O'Keefe, *Acta Crystallogr. B* 47 (1991) 192.
- [39] Y.N. Venetsev, V.V. Gagulin, *Ferroelectrics* 162 (1994) 23.
- [40] Y.N. Venetsev, V.V. Gagulin, I.D. Zhitomirsky, *Ferroelectrics* 73 (1987) 221.
- [41] H.W. Eng, P.W. Barnes, B.M. Auer, P.M. Woodward, *J. Solid State Chem.* 175 (2003) 94.
- [42] L.I. Shvorneva, Y.N. Venetsev, *Sov. Phys. JETP* 22 (1966) 722.
- [43] V. Bonny, M. Bonin, P. Sciau, K.J. Schenk, G. Chapuis, *Solid State Commun.* 102 (1997) 347.
- [44] A. Falqui, N. Lampis, A. Geddo-Lehmann, G. Pinna, *J. Phys. Chem. B* 109 (2005) 22967.
- [45] J.B. Goodenough, A. Wold, R.J. Arnett, N. Menyuk, *Phys. Rev.* 124 (1961) 373.
- [46] C. Malibert, B. Dkhil, J.M. Kiat, D. Durand, J.F. Berar, A. Spasojevic-de Bire, *J. Phys.: Condens. Matter* 9 (1997) 7485.